Chinese Chemical Letters 35 (2024) 109230

Contents lists available at ScienceDirect

Chinese Chemical Letters

journal homepage: www.elsevier.com/locate/cclet

Polyethylene imine functionalized porous carbon framework for selective nitrogen dioxide sensing with smartphone communication

Xiaxia Xing, Xiaoyu Chen, Zhenxu Li, Xinhua Zhao, Yingying Tian, Xiaoyan Lang, Dachi Yang*

Tianjin Key Laboratory of Optoelectronic Sensor and Sensing Network Technology, Engineering Research Center of Thin Film Optoelectronics Technology, Ministry of Education and Department of Electronics, College of Electronic Information and Optical Engineering, Nankai University, Tianjin 300350, China

ARTICLE INFO

Article history:
Received 18 July 2023
Revised 6 September 2023
Accepted 23 October 2023
Available online 25 October 2023

Keywords:
PEI/C framework
Nitrogen dioxide sensing
Enhanced selectivity
Smartphone communication
Practical monitoring simulation

ABSTRACT

Highly selective and remotely communicable nitrogen dioxide (NO_2) sensing may contribute to future Internet of Things in environmental monitoring. However, room-temperature NO_2 sensing materials such as carbon materials is still less than satisfactory due to their insensitive interaction with target gas. Here, polyethylene imine functionalized three-dimensional (3D) carbon framework (PEI/C framework) has been developed for enhanced selective NO_2 sensing, via combined template synthesis and subsequent doping. Typically, the 3D PEI/C framework is observed porous shape with irregular coating. Beneficially, the response of C framework to NO_2 increases while those of interfering gases decrease after being functionalized with PEI. Remarkably, the sensor prototypes show a 100 ppb-concentration detection limit at room temperature. Theoretically, such excellent NO_2 sensing is attributed to the large specific surface ratio of porous 3D PEI/C framework, in which PEI serves as an active layer for target NO_2, while a passivated one for interfering gases. Practically, such PEI/C framework sensor prototype is simulated for NO_2 sensing device and communicated with a smartphone, showing great potential in future intelligent environmental monitoring.

Nitrogen dioxide (NO_2) with toxicity and corrosiveness may cause photochemical smog and acid rain, seriously damaging the environment and threatening human health [1–3]. Specifically, NO_2 harms human respiratory tract, leading to chest tightness, dyspnea and even death [4,5]. Accordingly, the time-weighted average (TWA) exposure limit of NO_2 is 1 ppm and the threshold limit value is 3 ppm [6], in which selective detection and remote monitoring of low-concentration NO_2 are critically required.

The chemiresistive gas sensors are extensively utilized for detecting NO_2 due to their excellent portability [7] and sensing materials as a core component draw increasing attention. Among various NO_2 sensing materials, semiconducting metal oxides (SMOs) such as ZnO nanowalls [8], porous In_2O_3 nanosheets [9], Ni-doped SnO_2 nanofiber array [10], Fe-doped WO_3 films [11] and $Fe_2O_3/BiVO_4$ composites [12] have been investigated by exploring nanostructure, doping and constructing heterojunctions. Recently, two-dimensional transition metal dichalcogenide (TMDs) such as WS_2 [13], MoS_2 [14] and WSe_2/WS_2 [15] have been developed for room-temperature NO_2 sensing. Although great progress has been made, the power consumption of SMOs-built sensors and the response speed of TMDs need further improving. Especially, the above-reported strategies on boosting selectivity will simultaneously improve the responses of both target gas and interfering ones, which could lead to a decrease in interfering selectivity.

Carbon materials such as graphene and its composites show great application potential in room-temperature NO_2 sensing owing to their highly electrical conductivity and large specific surface areas [16,17]. However, the absorption of gas molecules on pristine carbon materials is determined to their weak van der Waals interaction, limiting their usage in highly selective and low-detection-limit gas sensing [18]. Actually, functionalized carbon materials with sensing dopants or nanostructures have been demonstrated to improve adsorption capabilities [19,20]. Nevertheless, it needs further exploration for a NO_2 sensing that could simultaneously possess high selectivity, low detection limit and fast response.

Ideally, the carbon materials with a large specific surface area are decorated by polymers accompanied with functional groups, which may be devoted to specific identification of target gas such as NO_2 while suppressing other interfering gases, however, few has been reported. In this study, a three-dimensional (3D) carbon framework functionalized with polyethylenimine (PEI/C framework, Figs. 1a and b) has been developed for selective NO_2

* Corresponding author.
E-mail address: yangdachi@nankai.edu.cn (D. Yang).

https://doi.org/10.1016/j.cclet.2023.109230
1001-8417/

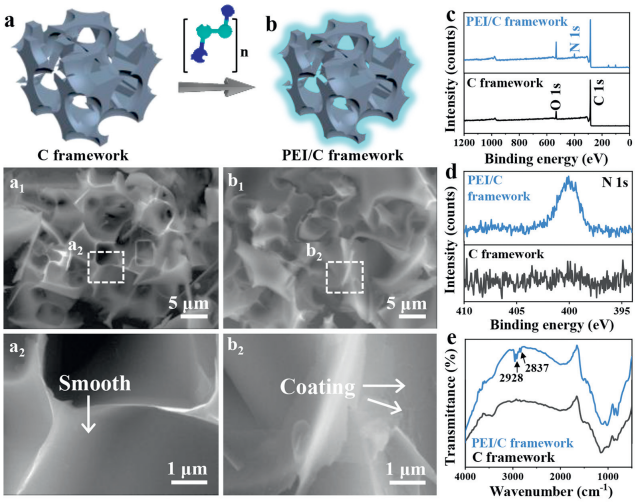

Fig. 1. (a, b) The schematic diagram on the synthesis of PEI/C framework. The SEM images of (a_1, a_2) C framework and (b_1, b_2) PEI/C framework by a closed magnification. (c) The XPS survey spectra, (d) high-resolution N 1s spectra and (e) FT-IR spectra of C framework and PEI/C framework.

sensing. Moreover, the detection limit of PEI/C framework was found as low as 100 ppb NO_2. Here, PEI/C framework and their-built sensor prototypes will be taken as examples in the following description.

In Figs. 1a_1 and a_2, the morphology of C framework was observed by scanning electron microscopy (SEM) and show porous 3D structure with smooth surface. Comparatively, the irregular coating was seen over the surface of 3D framework after introducing PEI in Figs. 1b_1 and b_2 and Fig. S1 (Supporting information). The various PEI/C frameworks are obtained by feeding various concentration of PEI in the precursor, however, it should be illustrated that the PEI content on C framework cannot be tuned. To further confirm the doping of PEI, X-ray photoelectron spectroscopy (XPS) was conducted. In Fig. 1c, the survey spectra of C framework show the peaks of C and O elements, while that of PEI/C framework present additional N element, which is the representative element of PEI and indicate the decoration of PEI on the C framework. Meanwhile, the high-resolution N 1s and C 1s spectra in Fig. 1d and Fig. S2a (Supporting information) is verified as well. In Fig. S2b (Supporting information), the high-resolution O 1s spectrum is deconvoluted into adsorbed oxygen (O_{ads}) and hydroxyl groups, in which O_{ads} of PEI/C framework possess higher proportion than that of C framework, contributing to the improved NO_2 sensing performance [21]. Moreover, the Fourier transform infrared spectroscopy (FT-IR) was performed in Fig. 1e, in which the FT-IR spectrum of PEI/C framework exhibits additional peaks at 2928 and 2837 cm^{-1} originating from PEI compared with that of C framework [22]. As a result, all the above characterizations reveal that the PEI is doped into C framework.

The PEI content-dependent NO_2 sensing was firstly evaluated at room temperature, the sensing resistance curves of pristine C framework and C framework functionalized with various content of PEI were shown in Fig. 2a, in which the pristine C framework presents poor response and recovery especially at higher concentration of 10 ppm NO_2. Remarkably, the response and recovery could be improved once introducing PEI, and the response value depend on the content of PEI on the C framework, especially the 10 mmol/L PEI/C framework exhibit the highest response to NO_2 in Fig. 2b and is thus taken as sample in the following demonstration. In Fig. 2c, the lower concentration of NO_2 was evaluated and the lowest detected content can reach ~100 ppb. Further, the response/recovery time of PEI/C framework to 5 ppm and 1 ppm NO_2 are evaluated of ~ 16.8 s/98.8 s and 33.5 s/208.7 s in Fig. 2d, respectively. Comparatively, the NO_2 sensing performances of various sensing materials at room temperature were summarized in Table S1 (Supporting information) [21,23–29], the PEI/C framework simultaneously presents advantages in low detection limit and fast response and recovery (Fig. 2e). In addition, the repetitive and

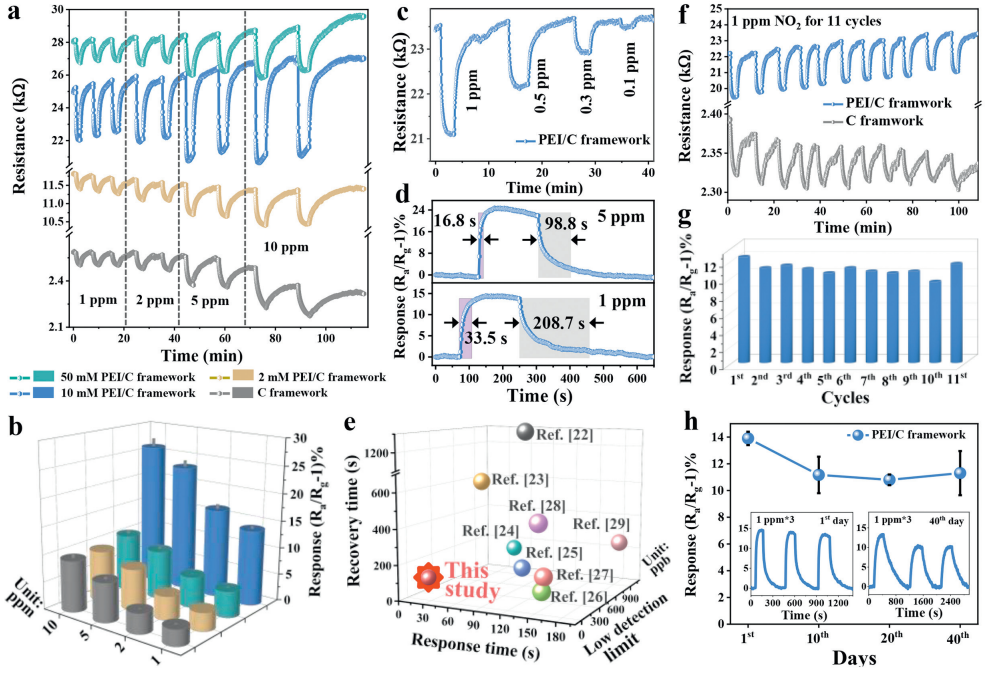

Fig. 2. (a, b) The comparison on NO_2 sensing performance between C framework and the one functionalized with various PEI. The real-time resistance curves of PEI/C framework to (c) 0.1–1 ppm NO_2. (d) The response and recovery time to 5 ppm and 1 ppm NO_2, respectively. (e) Comparison on low detection limit, response and recovery time with those of previous publications. (f) The real-time resistance curves of PEI/C framework and C framework to cycling 1 ppm NO_2. (g) The responses of PEI/C framework during 11 cycles. (h) The evaluation on long-term stability.

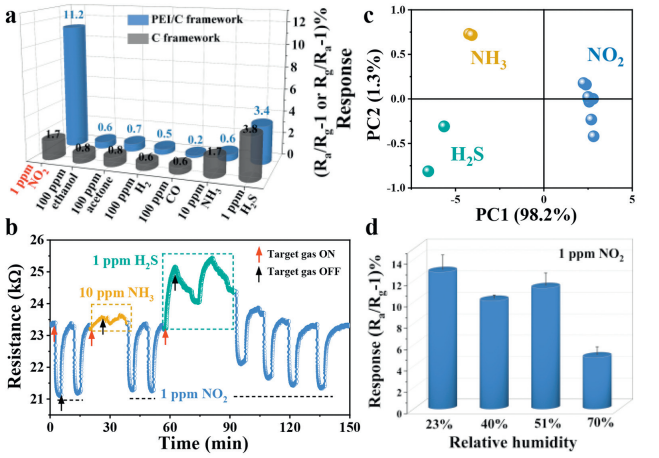

Fig. 3. (a) The comparison on selectivity between C framework and PEI/C framework. (b) The real-time resistance curve and (c) PCA analysis of PEI/C framework to target NO_2, interfering NH_3 and H_2S. (d) The comparison on sensing response to 1 ppm NO_2 at various relative humidity.

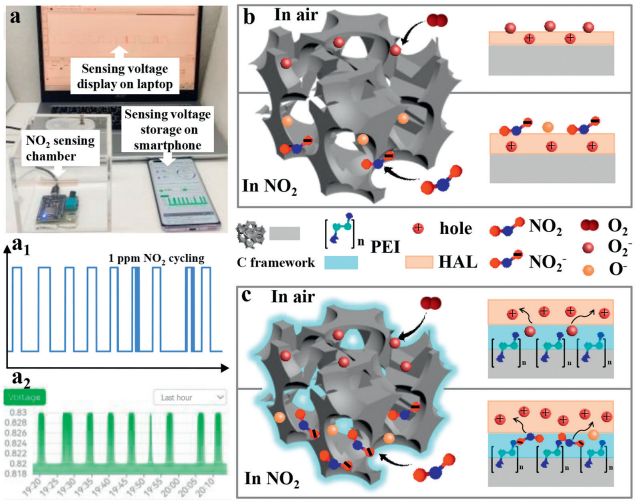

Fig. 4. (a) The photograph of sensing-response curve simultaneously displayed on the laptop and smartphone. The records of sensing voltage to cycling 1 ppm NO_2 on (a_1) laptop and (a_2) smartphone, respectively. The sensing mechanism schematic of (b) C framework and (c) PEI/C framework.

long-term stability are crucial parameters and were thus investigated. In Fig. 2f, the PEI/C framework presents better repeatability than that of C framework by cyclically testing 1 ppm NO_2, and the almost identical responses of PEI/C framework were summarized in Fig. 2g. Also, the 1 ppm NO_2 sensing performance of the same PEI/C framework sensor prototype during 40 days were evaluated and compared in Fig. 2h, which suggests excellent repeatability and reproducibility. It should be illustrated that the sluggish sensing response and recovery after 40 days may be attributed to the humidity and the interference from other molecules to PEI/C framework [30].

Selectivity is a vital parameter in sensing performance, which was evaluated by exposing the C framework and PEI/C framework to various gases with 100 ppm of ethanol, acetone, H_2 and CO, 10 ppm NH_3, 1 ppm of H_2S and NO_2 in Fig. S3 (Supporting information), respectively. The sensing response values were summarized in Fig. 3a, in which the pristine C framework possesses indistinguishable response to NH_3, H_2S and NO_2. Comparatively, PEI/C framework selectively increases the response of target NO_2 and decreases those of interfering gases such as NH_3 and H_2S. Further, we elaborately performed the NO_2 sensing evaluation of PEI/C framework after exposing it to the main interfering gases of NH_3 and H_2S in Fig. 3b, showing excellent anti-interference ability. Meanwhile, the principal component analysis (PCA) was carried out to distinguish the target NO_2 from interfering NH_3 and H_2S (Fig. 3c), which further verifies the excellent selective identification of PEI/C framework to NO_2. The detailed data of the above PCA are analyzed in Tables S2 and S3 (Supporting information). Additionally, the sensing performance of PEI/C framework to 1 ppm NO_2 at various humidity was studied in Fig. S4 (Supporting information) and the responses were compared in Fig. 3d, and one can see that the high environment humidity may affect NO_2 sensing. To further evaluate the reproducibility of the PEI/C framework sensor prototype in practical application, the NO_2 sensor device was constructed in Fig. S5 (Supporting information). When sensor module is powered by laptop, the acquired NO_2 sensing curve not only can be visualized on the smartphone but also on the laptop (Fig. 4a). Correspondingly, the cycling 1 ppm NO_2 sensing data was recorded on the laptop (Fig. 4a_1) and smartphone (Fig. 4a_2), respectively, showing excellent reliability of our simulated sensing device.

To understand the sensing mechanism of the PEI/C framework, the role of the pristine C framework was first investigated. In Fig. 2a, the C framework shows decreased sensing resistance when it was exposed to oxidizing NO_2 gas, which indicates the C framework possesses p-type semiconductor characteristic. Such phenomenon is verified by the Mott–Schottky (M–S) plot with a negative slope in Fig. S6 (Supporting information), depicting a typical p-type semiconductor nature (hole as the main carrier). Accordingly, the NO_2 sensing mechanism of C framework is diagramed in Fig. 4b. In air, the O_2 capture electrons from C framework to form adsorbed O_2^- (Eq. 1), increasing the surface hole concentration of C framework thus decreasing the resistance. In NO_2, the NO_2 will extract electrons from adsorbed oxygen ions on the surface of C framework (Eq. 2). Also, NO_2 directly capture more electrons from C framework (Eq. 3) to form adsorbed NO_2^- due to the stronger electron affinity of NO_2 than that of O_2 [27,31]. Both the above reactions generate more holes on p-type C framework, the NO_2 sensing with decreased resistance was observed.

$$O_2 + e^- \rightarrow O_2^- \quad (1)$$

$$NO_2 + O_2^- + 2e^- \rightarrow NO_2^- + 2O^- \quad (2)$$

$$NO_2 + e^- \rightarrow NO_2^- \quad (3)$$

Similarly, the NO_2 sensing mechanism of PEI/C framework is shown in Fig. 4c. It should be noted that the response of C framework to NO_2 increases while those of interfering gases decrease after being functionalized with PEI (Fig. 3a). Such phenomenon is entitled as "PEI serves as an active layer for target NO_2 while a passivated one for interfering gases", suggesting a boosted selectivity. Theoretically, PEI possess rich amine groups with electron-donating property serving as n-dopants to the p-type C framework [32,33], which is confirmed by the increased initial resistance of C framework after doping PEI (Fig. 2a). Therefore, the electrons transfer from the PEI/C framework surface to the NO_2 molecules due to the stronger electron affinity of NO_2 [27]. In this case, the PEI polymer acts as an active intermediate layer [34], promoting NO_2 sensing with fast response and recovery. On the contrary, if the PEI/C framework was exposed to the interfering gases such as H_2S and NH_3, which will react with pre-adsorbed oxygen species (O_2^-) to release electrons into PEI/C framework. However, the C framework has pre-received rich electrons from the donor of PEI, which may cause insensitivity to the extra electrons and thus decreased response to the interfering gases. As can be interpreted that PEI

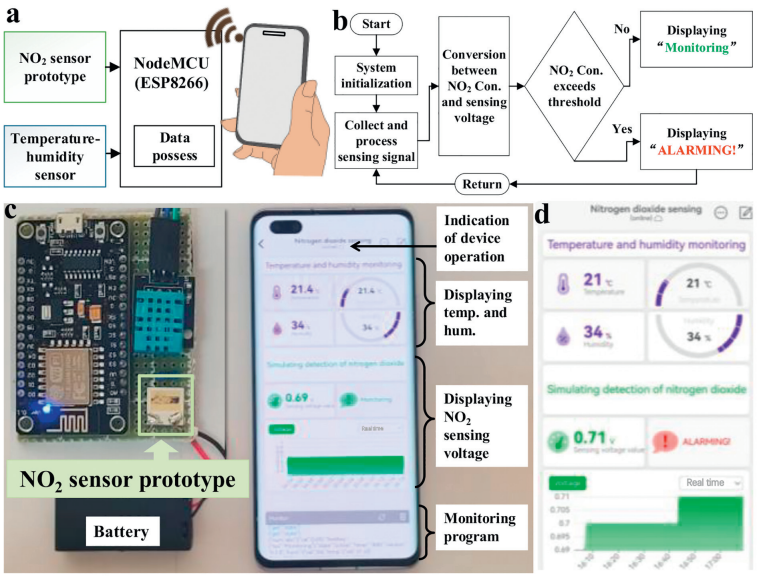

Fig. 5. (a) The block diagram of NO_2 monitoring and alarming device and (b) the corresponding flow diagram of alarm program. (c) The photograph of NO_2 monitoring and alarming device. (d) The real-time sensing data and alarming display on the smartphone.

acts as a passivated layer for the interfering gases. Accordingly, the PEI/C framework selectively enhances the sensing response to target NO_2, while decreasing the ones to those of interfering gases.

The NO_2 sensing was simulated by building the sensing device integrated PEI/C framework, communicating with a smartphone. Specifically, the PEI/C framework sensor prototype and temperature-humidity (temp.-hum.) sensor are connected to the microcontroller NodeMCU (ESP8266), which conducts Wireless Fidelity (Wi-Fi) communication between the sensors and smartphone, and the corresponding block diagram is schematized in Fig. 5a. Meanwhile, the NodeMCU performs the program to process the sensing data from PEI/C framework sensor prototype and temp.-hum. sensor, and to control the NO_2 alarming, the flow chart of the main program is shown in Fig. 5b. Notably, the NO_2 sensor prototype on the sensor module and the displayed information on the smartphone are marked in Fig. 5c. Experimentally, the alarming was simulated in the supplementary video, when 3 ppm NO_2 was injected and the sensing voltage reach alarm threshold, the smartphone shows red "AlARMING!" word (Fig. 5d). When the sensor module is placed in the air, the green "Monitoring" display on smartphone (Fig. 5c). Remarkably, as above presented sensor module powered by battery, the environmental temp.-hum. and NO_2 sensing data can be remotely monitored and updated in real-time by the smartphone.

To summarize, the enhanced selective NO_2 sensing has been developed with PEI/C framework *via* combined template synthesis and subsequent doping. Experimentally, the 3D PEI/C framework with porous morphology and irregular coating are observed. Theoretically, the PEI serves as an active layer for target NO_2 while a passivated layer for interfering gases, and the PEI/C framework possesses a large specific surface ratio (637 m^2/g, Fig. S7a in Supporting information). Beneficially, the sensor prototypes with PEI/C framework show excellent selectivity to NO_2, in which the response of C framework to NO_2 increases while those of interfering gases decrease after being functionalized with PEI. Moreover, the sensor prototypes present low detection limit of ~100 ppb NO_2 and a fast response time of 16.8 s to 5 ppm NO_2. As an example of application, the PEI/C framework has been integrated into a sensing device that communicates with a smartphone to simulate monitoring and alarming NO_2, which is potential in future intelligent sensing of Internet of Things.

Declaration of competing interest

The authors declare that they have no known competing financial interests or personal relationships that could have appeared to influence the work reported in this paper.

Acknowledgments

This work was financially supported by the National Natural Science Foundation of China (No. 52072184) and Tianjin Research Innovation Project for Postgraduate Students (General Project, No. 2022BKY035).

Supplementary materials

Supplementary material associated with this article can be found, in the online version, at doi:10.1016/j.cclet.2023.109230.

References

[1] M. Woellner, S. Hausdorf, N. Klein, et al., Adv. Mater. 30 (2018) 1704679.
[2] Z. Yang, H. Zou, Y. Zhang, et al., Adv. Funct. Mater. 32 (2022) 2108959.
[3] Z. Chu, M. Xiao, Q. Dong, et al., Chin. Chem. Lett. 34 (2023) 107197.
[4] L.B. Kreuzer, C.K.N. Patel, Science 173 (1971) 45–47.
[5] H.T. Huang, W.L. Zhang, X.D. Zhang, X. Guo, Sens. Actuator. B: Chem. 265 (2018) 443–451.
[6] K. Tian, X.X. Wang, H.Y. Li, et al., Sens. Actuator. B: Chem. 227 (2016) 554–560.
[7] M.E. Franke, T.J. Koplin, U. Simon, Small 2 (2006) 301.
[8] L. Yu, J. Wei, Y. Luo, et al., Sens. Actuator. B: Chem. 204 (2014) 96–101.
[9] L. Gao, Z. Cheng, Q. Xiang, et al., Sens. Actuator. B: Chem. 208 (2015) 436–443.
[10] W.T. Li, X.D. Zhang, X. Guo, Sens. Actuator. B: Chem. 244 (2017) 509–521.
[11] T. Tesfamichael, C. Piloto, M. Arita, J. Bell, Sens. Actuator. B: Chem. 221 (2015) 393–400.
[12] S. Bai, K. Tian, H. Fu, et al., Sens. Actuator. B: Chem. 268 (2018) 136–143.
[13] K.Y. Ko, J.G. Song, Y. Kim, et al., ACS Nano 10 (2016) 9287–9296.
[14] H.H. Hau, T.T.H. Duong, N.K. Man, et al., Sens. Actuator. A: Phys. 332 (2021) 113137.
[15] Y. Kim, S. Lee, J.G. Song, et al., Adv. Funct. Mater. 30 (2020) 2003360.
[16] J. Wu, Z. Li, X. Xie, et al., J. Mater. Chem. A 6 (2018) 478–488.
[17] T. Wang, X. Li, C. Li, et al., Sens. Actuator. B: Chem. 382 (2023) 133507.
[18] Y.R. Choi, Y.G. Yoon, K.S. Choi, et al., Carbon 91 (2015) 178–187.
[19] T.T. Tung, M.J. Nine, M. Krebsz, et al., Adv. Funct. Mater. 27 (2017) 1702891.
[20] W. Li, R. Chen, W. Qi, et al., ACS Sens. 4 (2019) 2809–2818.
[21] J.L. Fan, X.F. Hu, W.W. Qin, et al., J. Mater. Chem. C 11 (2023) 2364–2374.
[22] D.K. Singh, V. Kumar, V.K. Singh, S.H. Hasan, RSC Adv. 6 (2016) 56684–56697.
[23] M. Reddeppa, N.T. KimPhung, G.V. Murali, et al., Sens. Actuator. B: Chem. (2020) 129175.
[24] X. Chen, S. Wang, C. Su, et al., Sens. Actuator. B: Chem. 305 (2020) 127393.

[25] Y. Yang, D. Zhang, D. Wang, Z. Xu, J. Zhang, J. Mater. Chem. A 9 (2021) 14495–14506.
[26] D. Wang, D. Zhang, J. Guo, et al., Nano Energy 89 (2021) 106410.
[27] W. Zheng, Y. Xu, L. Zheng, et al., Adv. Funct. Mater. 30 (2020) 2000435.
[28] Z. Yang, D. Zhang, H. Chen, Sens. Actuator. B: Chem. 300 (2019) 127037.
[29] W. Yang, P. Wan, X. Zhou, et al., ACS Appl. Mater. Interfaces 6 (2014) 21093–21100.
[30] X. Xing, Z. Li, X. Chen, et al., ACS Appl. Mater. Interfaces 14 (2022) 17911–17919.
[31] Y. Su, G. Xie, H. Tai, et al., Nano Energy 47 (2018) 316–324.
[32] Y. Zhou, C. Fuentes-Hernandez, J. Shim, et al., Science 336 (2012) 327–332.
[33] S.-Y. Cho, K.M. Cho, S. Chong, et al., ACS Sens. 3 (2018) 1329–1337.
[34] S. Kumar, V. Pavelyev, P. Mishra, N. Tripathi, Bull. Mater. Sci. 43 (2020) 61.